PNAS
www.pnas.org

Supplementary Information for

Dissecting landscape art history with information theory

Byunghwee Lee, Min Kyung Seo, Daniel Kim, In-seob Shin, Maximilian Schich, Hawoong Jeong, Seung Kee Han

Hawoong Jeong
E-mail:hjeong@kaist.edu
Seung Kee Han
E-mail:skhan@chungbuk.ac.kr

This PDF file includes:

Supplementary text
Figs. S1 to S20
Tables S1 to S2
References for SI reference citations

www.pnas.org/cgi/doi/10.1073/pnas.2011927117

Supporting Information Text

I. Datasets

A. Data curation. Digital scans of landscape paintings were collected from the two major online sources: Wiki Art (WA) (1) and the Web Gallery of Art (WGA) (2). For our purpose, we collected 12,431 landscape paintings by 1,071 artists assigned to 61 nationalities from WA, and 3,610 landscape paintings by 816 artists assigned with 20 nationalities from WGA. While the overall number of paintings from WGA is relatively smaller than from WA, the WGA dataset has a larger volume of paintings produced before 1800 CE. Therefore, we utilize both datasets in a complementary way.

As same paintings can be included in both datasets, we carefully constructed a unified dataset by filtering out the duplicate paintings from both datasets by using meta-information of paintings (title, painter, completion date, etc.) to construct a unified set of painting images. The filtering process is as follows. We first found 133 painters commonly exist in the two datasets. For the 3,004 paintings corresponding to these painters in WGA, we compared each painting image with the painting images produced from the same painter in the WA dataset. 949 duplicate paintings were removed from WGA, and combining it with WA resulted in a unified set consisting of 15,092 distinct paintings from 1,483 landscape painters. We further filtered out 176 painting images that deemed improper for our analyses as shown in the sample in Fig. S1. The improper images include paintings with curved frame, Chinese fan shape paintings, tilted paintings, paintings from different genres, ambiguity in frame, etc. (See the sample images in Fig. S2). For the painting images that contains a rectangular frame or boundary, we manually cropped out the frame to keep only pure painting image. Though the used partitioning algorithm is affected very little by the size of an image, the lengths of the longer sides of the painting images were set to 400 pixels, while preserving their aspect ratios, so that all the images are of similar size. The final dataset after whole pre-processing procedure consists of 14,912 landscape paintings from 1,476 artists.

We also collected 5,780 abstract paintings by 175 painters from WA dataset in a separate auxiliary dataset. The abstract painting dataset includes artworks by abstract painters in the three WA categories: 'abstract art', 'post-painterly abstraction', 'abstract expressionism'. Similarly to the landscape dataset, from originally 7,429 paintings, we also filtered out improper images such as images with ambiguous frame, pictures of 3D objects, resulting in a total of 5,780 paintings. List of all used landscape and abstract paintings are provided in the SI datasets with corresponding metadata. Table. S1 summarizes the total dataset over time periods. Figure S3 shows the number of paintings and painters in different nationalities over time. The number of paintings by conventional style periods in the two dataset is shown in the Fig. S4.

B. Nationality of artists. To have a consistent nationality attribution for each artist, we newly collected nationality information for all artists in WGA dataset from English Wikipedia (4) because artist information of WA dataset, which contributes to a larger volume of the combined dataset, refers to Wikipedia information. For artists who have explicit 'nationality' category in their personal biography cards in their Wikipedia page, we used the nationality information. For the remaining artists who have no 'nationality' category in their biography cards, we extracted the information from the first paragraph of the artists' Wikipedia description pages such as "*Artist* ... was a *Nationality* painter.". If an artist is assigned to multiple nationalities, we consistently chose the first or birth nationality as taking into account multiple nationalities would raise confusion between nationalities. Consequently, all paintings by each artist are assigned to a single nationality according to the artist's nationality. Figure S3 A summarizes the number of paintings and artists in each nationality in every 50-year time-bins from 1500 CE to 2000 CE. To check whether the number of paintings in each nationality coherent to the amount of current literature related to each nationality, we independently investigated the number of landscape painting books related to each nationality in WorldCat, which is a large online library catalog service (5). We note that there are significant positive correlations between the number of paintings (and artists) of nationalities in the dataset and the number of books found in WorldCat (Pearson coefficient, $\rho \approx 0.50$ and $\rho \approx 0.48$ for paintings and artists respectively with $P < 0.001$).

C. Bias in datasets. Regarding artists' nationalities, we acknowledge that general literature on landscape painting art history and how-to books do avoid the "nationality" issue since several decades. Yet, our dataset shows that there is a memory effect in the system, as WA, WGA, Wikipedia, and large library catalogs such as WorldCat still assign or keep assignments of nationality to landscape paintings in a prominent way.

We also note that as the collected datasets are male-dominated data sets, female landscape painters could be under-represented than the male painters. We acknowledge that our dataset is preliminary and we welcome the collection and inclusion of more female artists in large datasets.

II. Methodology

Partitioning image using compositional information. In this section, we introduce the information-theoretic methodology for finding partitioning positions in images based on Rigau *et al.*'s image partitioning algorithm. In the case of Rigau's original algorithm, the algorithm decides a dissection position by looking for a set of sub-regions in the image which produce maximum mutual information between the color palette of an original image and the palette of candidate sub-regions (6). More recently, Shin *et al.* introduced a more efficient method for computing the compositional information called the line-updating bi-partitioning (LUB) algorithm (7) (published in Korean). The LUB algorithm on average reduces the time complexity for finding a dissection position in an image by the length of the image. Therefore the LUB algorithm is essential for analyzing recent large-scale high-resolution images. Here we first explain how a partitioning position is determined by the mutual information and introduce how the LUB algorithm works in detail.

The partitioning algorithm progressively subdivides an image according to the partitions which provide maximum information gain at each step. For a random variable C taken from the set of discrete colors used in a visual image, the palette information of the image is defined as the Shannon entropy $H(C)$:

$$H(C) = -\sum_{c \in C} P(c) \log_2 P(c) \quad [1]$$

where the probability $P(c)$ is given by $P(c) = S_c/S$ where S_c denotes the number of pixels taking color c, and S is the size of the image.

Taking the process of painting as a mapping from a palette of color set C to a set R composed of a finite number of regions in a canvas, the conditional entropy $H(C|R)$ is defined as:

$$H(C|R) = -\sum_{c \in C, i=1,2} P(c, r_i) \log_2 P(C|R = r_i). \quad [2]$$

Here the conditional probability $P(c|r_i)$ is the probability of color c in region r_i and the joint probability is $P(c, r_i) = P(c|r_i)P(r_i)$ where $P(r_i) = \pi_i = s_i/S$ is size of the region r_i normalized by the full size S. Then, the information gained from introducing a partition with a set of two sub-regions R is expressed by the mutual information:

$$\begin{aligned} I(C, R) &= H(C) - H(C|R) \\ &= H(C) - [\pi_1 H(C, r_1) + \pi_2 H(C, r_2)], \end{aligned} \quad [3]$$

where the regional Shannon entropy $H(C_i, r_i)$ for the color set C_i in the region r_i is given by:

$$H(C_i, r_i) = -\sum_{c \in C_i} P(c|r_i) \log_2 P(c|r_i). \quad [4]$$

During the first partition process, one should calculate the compositional information gain over all possible partitions in both horizontal and vertical directions on the entire image resulting in $w - 1 \times h - 1$ trials, where w and h is the number of pixels of weight and height of the image. Then the algorithm select a partition which gives the maximum information. From the second partitioning process, the algorithm is repeatedly applied to remaining sub-blocks and partition sub-blocks at the positions that offer maximum information. In principle, the partitioning process can be continued until the image is fully decomposed into regions of homogeneous colors.

During the scanning process for finding the optimal dissection position, the conventional method newly calculates compositional information for every possible partitioning line. For instance, in Fig. S5, the compositional information from the partition at the $k+1$th line is calculated independently to the kth line in the conventional algorithm. However, a large portion of the calculation at the $k+1$th step has overlap with the previous kth step. Using the LUB algorithm, one reduces the redundant process in calculating the compositional information at the $k+1$th pixel by utilizing previously calculated palette information at the kth pixel.

When the partitioning position is updated from $y = k$ to $y = k+1$, one should both calculate the palette information of extended region r'_1 and the reduced region r'_2 (Fig. S5 B). The essence of LUB algorithm is to express the new palette information $H(C, r'_1)$ and $H(C, r'_2)$ in terms of previously calculated $H(C, r_1)$ and $H(C, r_2)$. For the calculation of $H(C, r'_1)$, we define the color variables of r'_1 into three categories.

- C_0: Colors that are included in the region r'_1 but belongs only to the previous region r_1.
- C_m: Colors that are in both r_1 and r_{line}.
- C_a: Colors that are only in r_{line}.

If the width and the height of an image is given as L_x and L_y, the area of region r'_1 is $L_x(k+1)$. If the number of pixels of color c in R_1 is $N(c)$ and the number of pixels of color c in the line is $n(c)$, $H(C, r'_1)$ can be expressed by the summation of information of three color variables.

$$H(C, r'_1) = -\sum_{c \in C_0} \frac{N(c)}{L_x(k+1)} \log_2 \frac{N(c)}{L_x(k+1)} - \sum_{c \in C_m} \frac{N(c)+n(c)}{L_x(k+1)} \log_2 \frac{N(c)+n(c)}{L_x(k+1)} - \sum_{c \in C_a} \frac{n(c)}{L_x(k+1)} \log_2 \frac{n(c)}{L_x(k+1)} \quad [5]$$

and $H(C, r_1)$ can be expressed as,

$$
\begin{aligned}
H(C,r_1) &= -\sum_{c\in C_0}\frac{N(c)}{L_x k}\log_2\frac{N(c)}{L_x k} - \sum_{c\in C_m}\frac{N(c)}{L_x k}\log_2\frac{N(c)}{L_x k} \\
&= -\frac{K+1}{k}\sum_{c\in C_0}\frac{N(c)}{L_x(k+1)}\log_2\frac{N(c)}{L_x(k+1)} - \sum_{c\in C_0}\frac{N(c)}{L_x k}\log_2\frac{K+1}{k} - \sum_{c\in C_m}\frac{N(c)}{L_x k}\log_2\frac{N(c)}{L_x k}.
\end{aligned}
\tag{6}
$$

From Eq.6, we get

$$
-\sum_{c\in C_0}\frac{N(c)}{L_x(k+1)}\log_2\frac{N(c)}{L_x(k+1)} = \frac{k}{k+1}H(C,r_1) + \sum_{c\in C_0}\frac{N(c)}{L_x(k+1)}\log_2\frac{k+1}{k} + \sum_{c\in C_m}\frac{N(c)}{L_x(k+1)}\log_2\frac{N(c)}{L_x k}. \tag{7}
$$

Substituting Eq.7 into Eq.5, we can express $H(c,r_1')$ in terms of $H(c,r_1)$ using the following relation:

$$
\begin{aligned}
H(C,r_1') = \frac{k}{k+1}H(C,r_1) - \frac{k}{k+1}\log_2\frac{k}{k+1} - \sum_{c\in C_m}\frac{N(c)+n(c)}{L_x(k+1)}\log_2\frac{N(c)+n(c)}{L_x(k+1)} \\
+ \sum_{c\in C_m}\frac{N(c)}{L_x(k+1)}\log_2\frac{N(c)}{L_x(k+1)} - \sum_{c\in C_a}\frac{n(c)}{L_x(k+1)}\log_2\frac{n(c)}{L_x(k+1)}.
\end{aligned}
\tag{8}
$$

In similar manner, the palette information $H(c,r_2')$ of the bottom region r_2' can be obtained using $H(c,r_2)$. Again we define three color variables in r_2' (Fig. S5).

- C_0: Colors that are only belongs to the region r_2'.
- C_m: Colors that are in both r_2' and r_{line}.
- C_d: Colors that are only in r_{line}.

Defining the number of color c in r_2 as $N(c)$ and the number of color c in the r_{line} as $n(c)$, $H(C,r_2)$ and $H(C,r_2')$ are expressed by the summation of information terms of the three color variables.

The palette information of r_2' is

$$
H(C,r_2') = -\sum_{c\in C_0}\frac{N(c)}{L_x(L_y-(k+1))}\log_2\frac{N(c)}{L_x(L_y-(k+1))} - \sum_{c\in C_m}\frac{N(c)-n(c)}{L_x(L_y-(k+1))}\log_2\frac{N(c)-n(c)}{L_x(L_y-(k+1))}, \tag{9}
$$

and the palette information of r_2 is

$$
H(C,r_2) = -\sum_{c\in C_0}\frac{N(c)}{L_x(L_y-k)}\log_2\frac{N(c)}{L_x(L_y-k)} - \sum_{c\in C_m}\frac{N(c)}{L_x(L_y-k)}\log_2\frac{N(c)}{L_x(L_y-k)} - \sum_{c\in C_d}\frac{n(c)}{L_x(L_y-k)}\log_2\frac{n(c)}{L_x(L_y-k)}. \tag{10}
$$

Expanding the logarithmic term using

$$
\log_2\frac{N(c)}{L_x(L_y-k)} = \log_2\frac{N(c)}{L_x(L_y-(k+1))} + \log_2\frac{L_y-(k+1)}{L_y-k}, \tag{11}
$$

and substituting Eq.10 into Eq.9, we get the following relation.

$$
\begin{aligned}
H(C,r_2') = \frac{L_y-k}{L_y-(k+1)}H(C,r_2) - \frac{L_y-k}{L_y-(k+1)}\log_2\frac{L_y-k}{L_y-(k+1)} - \sum_{c\in C_m}\frac{N(c)-n(c)}{L_x(L_y-(k+1))}\log_2\frac{N(c)-n(c)}{L_x(L_y-(k+1))} \\
+ \sum_{c\in C_m}\frac{N(c)}{L_x(L_y-(k+1))}\log_2\frac{N(c)}{L_x(L_y-(k+1))} + \sum_{c\in C_d}\frac{n(c)}{L_x(L_y-(k+1))}\log_2\frac{n(c)}{L_x(L_y-(k+1))}.
\end{aligned}
\tag{12}
$$

Then, the new compositional information for partitioning at $k+1$th line is calculated with the Eq. 3.

Fig. S6 compares the calculation time to find the first partition in randomly generated 3-bit images depending on partitioning algorithms. The LUB algorithm approximately reduces the time complexity by the length of an image ($\approx S^{1/2}$). In other words, for a square image with the length of 1,000 pixels (1,000,000 pixels in the total area), the LUB algorithm is approximately 1,000 times faster than the conventional method.

III. Effect of color depth, size, and aspect ratio on the partitioning process

Effect of color depth and image size on the image partitioning process. An image represented with high color depth where large number of bits are used to represent a color of a pixel looks more natural and realistic to human vision. However, because the partitioning process employed in this study considers each color component a discrete variable resulting in that colors of slight differences to be considered completely different colors even though they are not sensitively differentiated by normal human eyes. Therefore, in this study, we use painting images which are coarse-grained in the RGB color space. The analyses in the main article were conducted on the images of 3-bit color depth (1-bit for each R,G,B values), which is the simplest coarse-grained form to represent an image in the RGB color space (Fig. S7). To produce 3-bit painting images, we find a set of median values for each of R, G, B components for each painting as threshold values. Then, RGB components of a pixel of an image are transformed into one if they are above or equal to the threshold, or zero if they are below the threshold. We also verified that other low color depth systems such as 3-bit images obtained from different threshold condition (instead of using the medians we choose 128 as an absolute threshold among 256 values in each R, G, B values), 8-bit (256 colors) images, and 8-bit gray-scale images provide similar and robust results.

Another advantage of using low color depth system in the partitioning analysis is that it eliminates finite-size effects of sub-blocks of an image to the compositional information during the partitioning process. Consider an image of fixed size composed of various colors. In an extremely high color-depth, two colors of slight differences are considered to be distinct colors. Therefore, the palette information $H(C)$ of the image, which is the Shannon entropy of color distribution, is found to be similar to the case of a randomly colored image. For a random finite size image where all pixels have different color variables, the partitioning process in high color depth representation leads an image to be partitioned at $1/2$ position. This is because the size effect of sub-blocks intervenes into the partitioning process as follows. The partitioning algorithm finds the dissection position of an image that gives the maximum compositional information:

$$I(C,R) = H(C) - [\pi_1 H(C|R_1) + \pi_2 H(C|R_2)], \qquad [13]$$

where $H(C)$ is the original color palette information, and π_1 and π_2 are the proportion of each sub-block R_1 and R_2 to the original block ($\pi_1 + \pi_2 = 1$). In the case of high color-depth limit, the available number of distinct colors N_c is much larger than the number of pixels of an image S ($N_c \gg S$). Then the information terms are approximated as $H(C) \approx \log_2(S)$, $H(C_1|R) \approx \log_2(\pi_1 S)$ and $H(C_2|R) \approx \log_2(\pi_2 S) = \log_2((1-\pi_1)S)$ resulting in

$$\begin{aligned} I(C,R) &= \log_2 S - \pi_1 \log_2 \pi_1 S - \pi_2 \log_2 \pi_2 S \\ &= \log_2 S - \pi_1 \log_2 S - \pi_2 \log_2 S - \pi_1 \log_2 \pi_1 - \pi_2 \log_2 \pi_2 \\ &= -\pi_1 \log_2 \pi_1 - (1-\pi_1)\log_2(1-\pi_1). \end{aligned} \qquad [14]$$

Therefore, the compositional information $I(C,R)$ is maximized at $\pi_1 = 1/2$ and 1 bit of information is obtained by the partition (Fig. S8).

At the opposite limit where the size of an image is sufficiently larger than the number of distinct colors ($N_c \ll S$), a randomly colored image has its palette information $H(C) \approx H(C|R_1) \approx H(C|R_2)$. Therefore, the compositional information $I(C,R)$ becomes almost zero over any π_1. In other words, partitioning can take place at any position on a painting (or no preferred position is found, Fig. S8).

Since we don't expect a randomly colored painting to be partitioned at the center position (i.e., it means that there is a particular preference at the proportion of $1/2$ for a painter who randomly paints), a coarse-graining process of a painting in the color space is necessary to eliminate this size effect. The 3-bit color depth system we take in this study is the simplest form to represent (R,G,B) values and satisfies the condition $N_c \ll S$.

We provide detailed statistics of image size and color palette information for the used dataset in the Fig. S9. The original digital scans of paintings are represented in the 24-bit RGB color representation. The average number of unique colors used in a painting image in the dataset is 89,063 and the typical color palette information is 14.6 bit, indicating that effectively $N_c = 2^{14.6} \approx 24,834$ colors are used for a typical landscape painting image. The average image size of the landscape paintings is 461,304 pixels. Since the order of magnitude of typical number of colors in a painting image is not sufficiently small compared to the painting size, analyses in high color depth systems such as 24-bit or 16-bit color system could cause the size effect discussed above.

Robustness of the results from different color depth images. To check the robustness of the results in the main manuscript, we independently conducted the same analyses on four different types of color depths: 3-bit images obtained from median threshold (result used in the main manuscript), 3-bit images from absolute threshold, 8-bit color images, and 8-bit gray-scale images. Results of the analyses including the distribution of partition direction up to second partition (Fig. S10), the changing trend of the distribution of r_c over time (Fig. S11 and S12) were found to show similar overall behavior.

Effect of aspect ratio on partitioning position. The majority of partitions in the early partition steps of landscape paintings is partitioned in horizontal direction (Fig. S13 B). 86.8% of paintings are horizontally partitioned at the first partition with larger compositional information compared to vertically partitioned cases. After approximately 10 partition steps, the probability of a painting to be partitioned in horizontal direction begins to saturate at the point slightly above 0.5. However, in case of the abstract paintings, the probability of partition direction merely changes over all partition steps implying no directional preference in composition (Fig. S13 H).

It is interesting that the proportion of vertical partition saturates at slightly above 0.5 up to 100 partition steps. One possible cause of the effect is that the width of an image is larger than the height on average (Fig. S13 A and E). An image with longer width than height naturally has more chance to be partitioned vertically. To test whether this hypothesis is true, we divided landscape and abstract painting dataset into two groups where one group has longer width and the other group has longer height. In case of abstract paintings that have longer width than height (Fig S13 G), the proportion of vertically partitioned painting was larger. However, for the group of abstract paintings that has longer height than their width, the proportion of horizontal partition was almost similar or slightly smaller than the proportion of vertical partition after 10 partition steps. On the contrary, in case of landscape paintings, the proportion of vertical partition was always larger after 10 partition steps for any group of paintings though the effect was moderate for longer height images. Therefore, aspect ratio of painting images only partly explains the asymmetry in the proportion of partition direction at the higher partition steps.

We speculate that the vertical objects in landscape paintings could cause the remaining asymmetric effect. Whereas large scale objects in landscape paintings such as sky, earth, and ocean are horizontally painted, relatively smaller objects such as trees, plants, and buildings are vertically placed. Therefore, the frequent existence of vertically oriented objects in landscape paintings could cause the distinguishing characteristic in the profile of partition direction when compared to abstract paintings.

IV. Analysis of composition in landscape paintings based on partition directions across nationalities

The distribution of composition based on first and second partition directions differs significantly by partition types (H–H, H–V, V–H, and V–V). Figure.2C in the main manuscript shows that the relative frequency of each composition type gradually changes over time while the trend is transcending concepts of nationalities. Fig. S14 shows detailed distributions of partition types of the dominant individual nationalities with more than 30 paintings, for five time periods. The five time periods were set to contain same number of paintings in each time-bin. As shown in Fig.2B and C in the main manuscript, we observe a transition in the proportion of composition types during the mid-nineteenth century; H–H type composition becomes more dominant since the mid-nineteenth century.

V. Selection criterion used for representative individual artists

For the analysis on the distribution of dissection proportions of individual painters, we filtered out 134 individual painters whose number of paintings is within top 10% of the dataset before and after 1800 CE, resulting in 31 and 103 painters from two periods respectively. We introduce this separate criterion because the number of paintings of individual painters begins to increase largely from 1800 CE, therefore applying a uniform selection criterion in the whole periods would possibly cause a selection bias towards the modern era. Figure S15 shows the sudden increase in the number of paintings from 1800 CE.

VI. Proportion-similarity network

Figure. S16, S17, and S18 shows the enlarged versions of matrix representation of the proportion-similarity networks between and among individual artists and conventional style periods in the Fig. 4 of the main manuscript. Table S2 shows the list of artists in each community. Figure S19 and S20 shows the one-mode projection of the bipartite network (Fig. 4A) onto the individual artists and the conventional style periods.

Figure and Tables

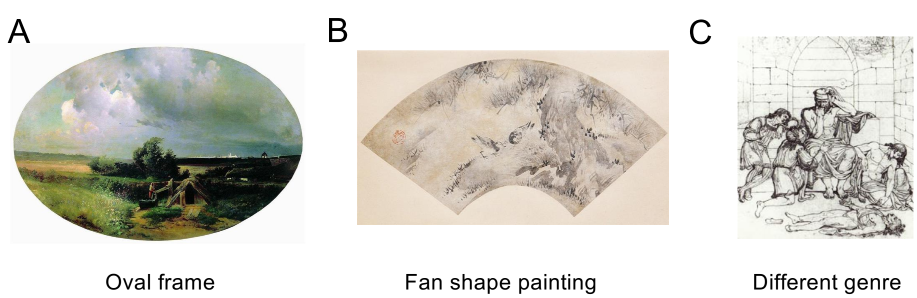

Fig. S1. Sample paintings that deemed improper for the analysis. During the data pre-processing period, we filtered out the inappropriate paintings for applying our partitioning algorithm. A-C: Painting image credit: WikiArt

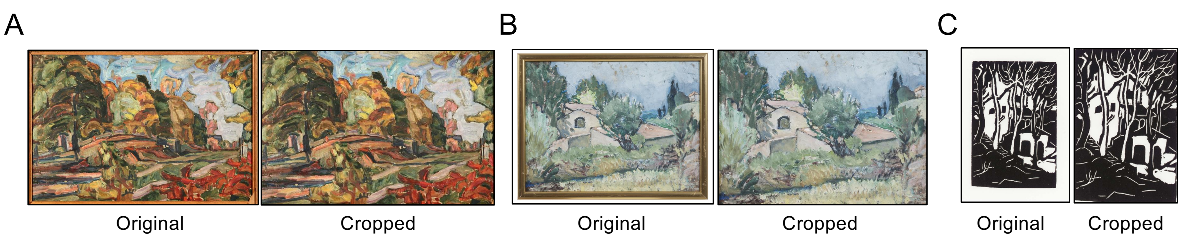

Fig. S2. In the original data set, 998 paintings with rectangular frame were included. We cropped out the frames of the painting images to keep only pure painting images. A-C: Painting image credit: WikiArt

Table S1. Summary of the painting data set. Overall, 14,912 landscape paintings from 1,476 artists were analyzed in this study. 1,470 abstract paintings were also assessed for the comparison purpose.

Category		WGA		WA		Unified	
	Year	# paintings	# painters	# paintings	# painters	# paintings	# painters
Landscape painting	-1500	-	-	57	10	47	9
	1501-1600	147	38	79	14	150	44
	1601-1650	667	155	245	27	625	123
	1651-1700	648	117	101	16	585	131
	1701-1750	345	65	84	10	305	49
	1751-1800	355	83	221	25	516	86
	1801-1850	399	125	1,094	87	1306	184
	1851-1900	1 049	234	3 879	287	4522	425
	1901-1950	-	-	5 065	510	5245	543
	1951-2000	-	-	1 335	244	1335	247
	2000-	-	-	271	56	276	57
	Total	3 610	816	12 431	1 071	14 912	1,476
		# paintings	# painters				
Abstract painting		1 470	19				

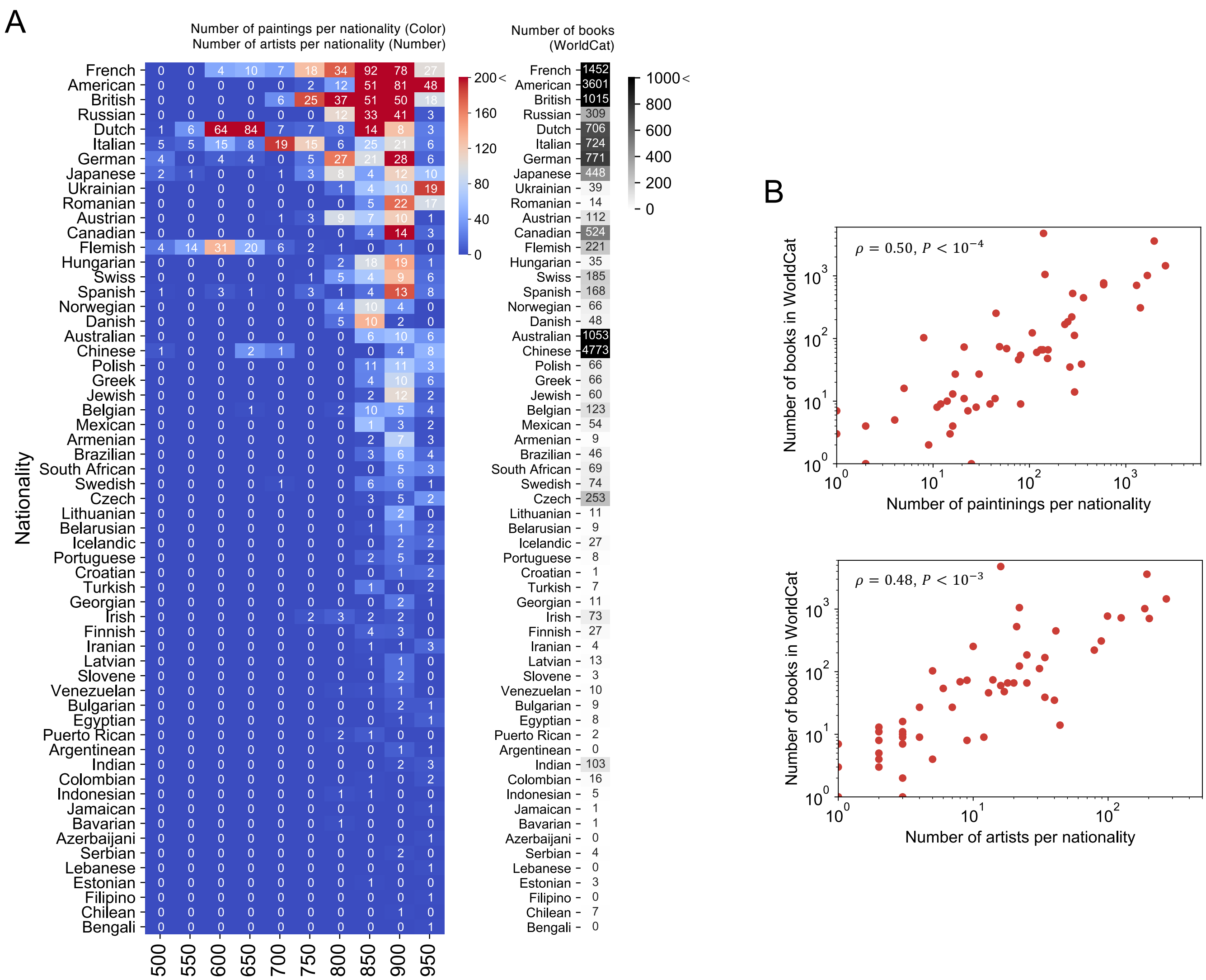

Fig. S3. (A) The heatmap shows the number of landscape paintings and painters for 59 nationalities in 50-year time periods. Colors indicate the number of paintings and the numbers indicate the number of artists. The heatmap on the second column represents the number of books in WorldCat related to each nationality. (B) shows that there are significant positive correlations between the number of paintings and paintings, and number of books in WorldCat.

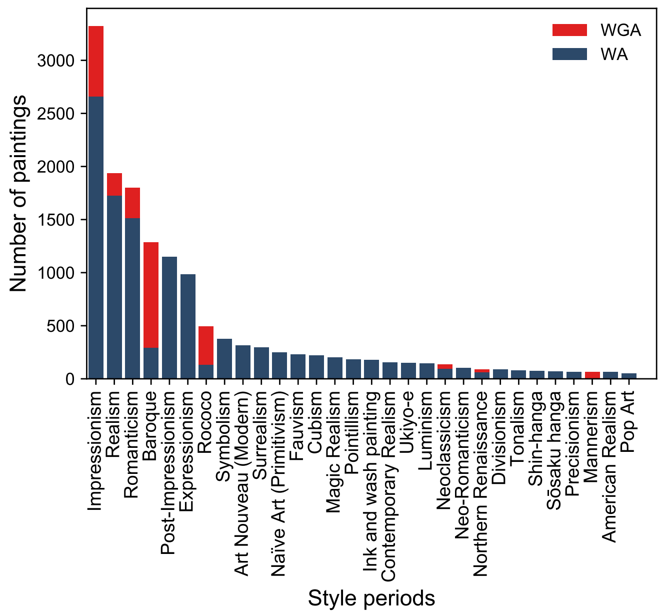

Fig. S4. The number of paintings by conventional style periods in the dataset. Top 25 style periods which have largest number of paintings are shown on the graph. Number of paintings from different data sources are depicted by different colors: WA in blue and WGA in red.

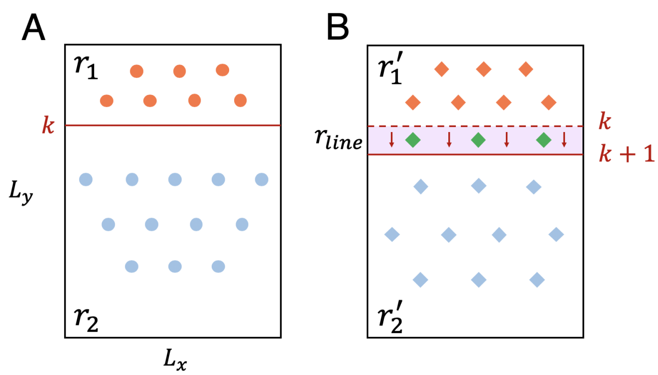

Fig. S5. A schematic description on the partitioning process using the LUB algorithm. The LUB algorithm calculates the mutual information obtained from a horizontal partition at position $y = k + 1$ based on the information gain at $y = k$.

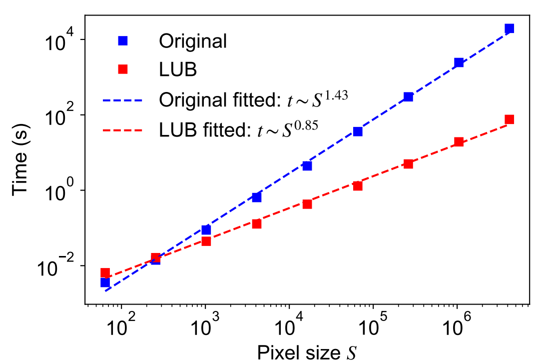

Fig. S6. Calculation time to find the first partition in a 3-bit random image depending on partitioning algorithms. The LUB algorithm reduces the time complexity approximately by the length of an image ($\approx S^{1/2}$).

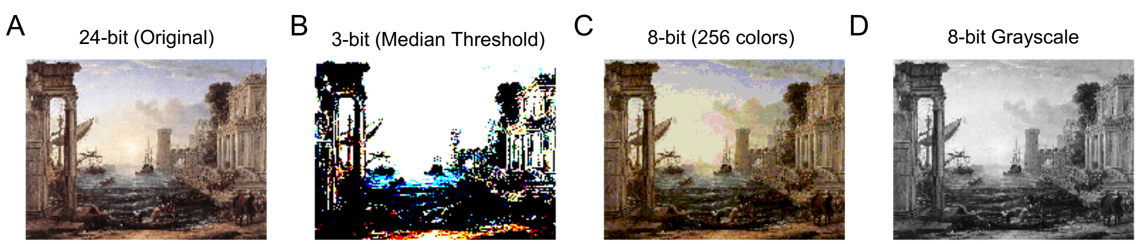

Fig. S7. Sample painting (Claude. Seaport with the Embarkation of the Queen of Sheba. 1648) transformed into different color-depth images: (A) 24-bit (original), (B) 3-bit, (C) 8-bit, (D) 8-bit gray-scale respectively. Painting image credit: The National Gallery.

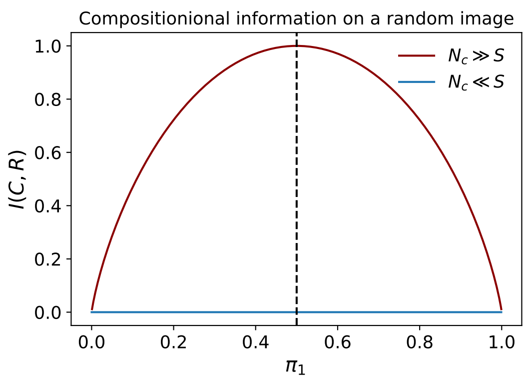

Fig. S8. The compositional information $I(C, R) = -\pi_1 \log_2 \pi_1 - (1 - \pi_1) \log_2 (1 - \pi_1)$ in Eq. 14 as a function of π_1 in high-color depth limit ($N_c \gg S$) is expressed in the dark red. The compositional information for the case of $N_c \ll S$ is depicted by the blue line.

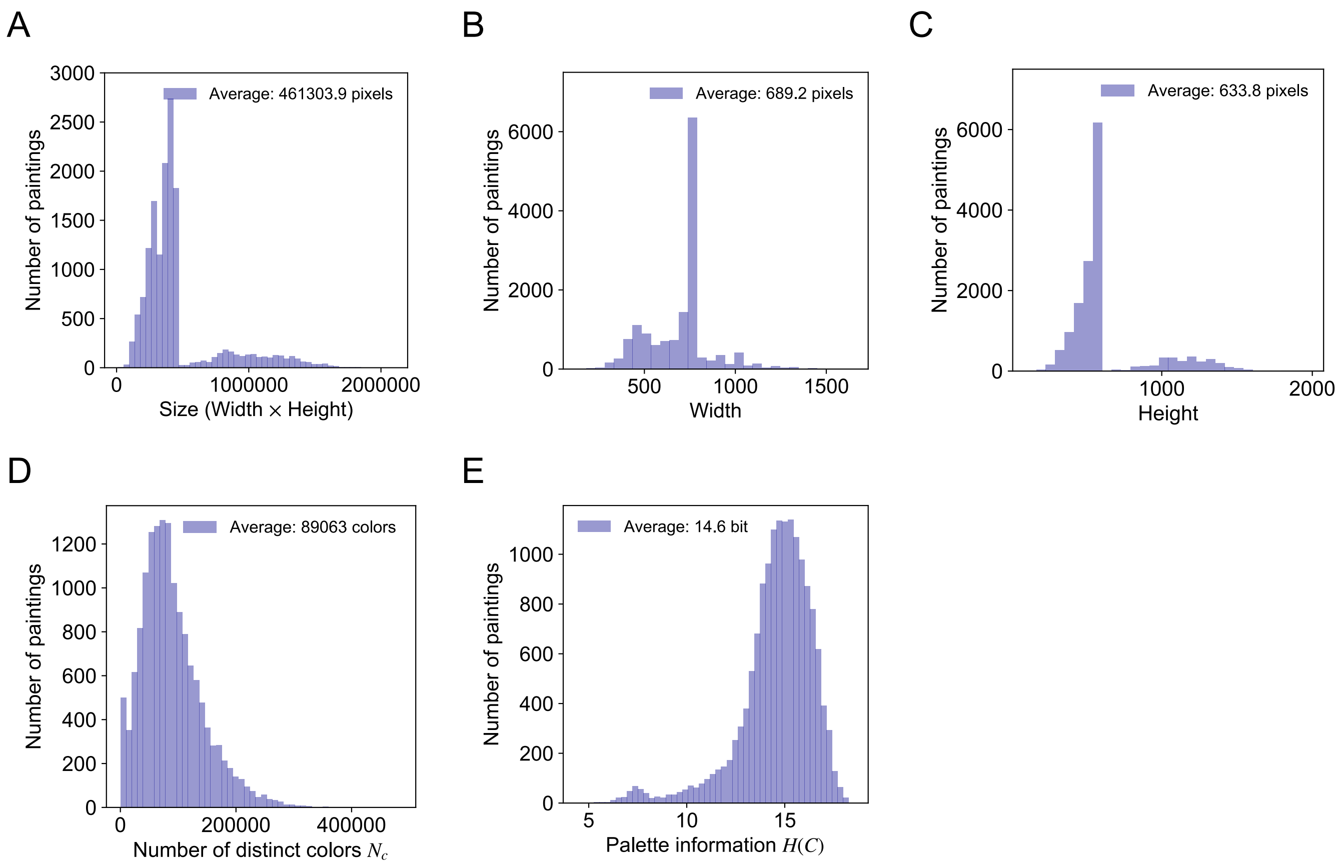

Fig. S9. Basic statistics of landscape painting images. Distribution of (A) image size, (B) width, (C) height, (D) Distinct number of colors N_c, and (E) the palette information $H(C)$.

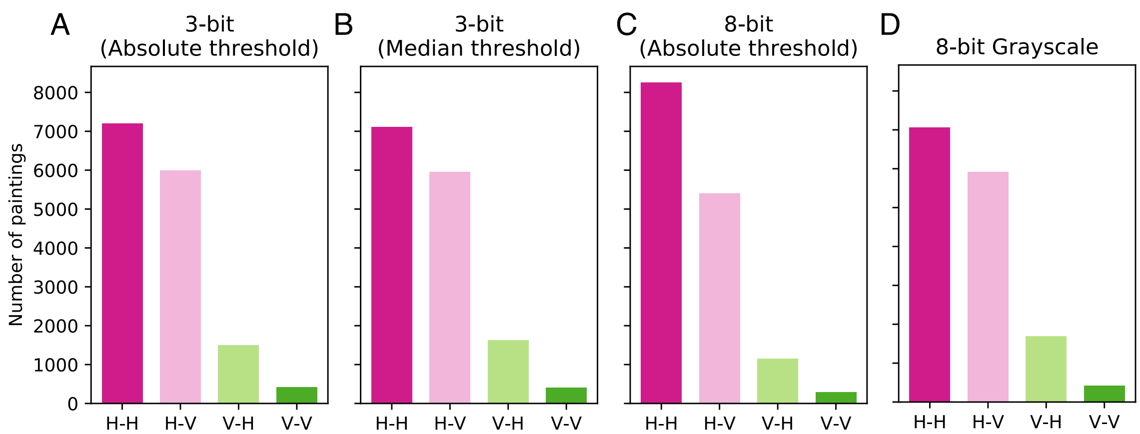

Fig. S10. Histograms of directional preference up to second partition step by color depth: (A) 3-bit (absolute threshold), (B) 3-bit (median threshold), (C) 8-bit (absolute threshold), and (D) 8-bit grayscale. Overall pattern of the distributions are similar and robust under different color depth condition.

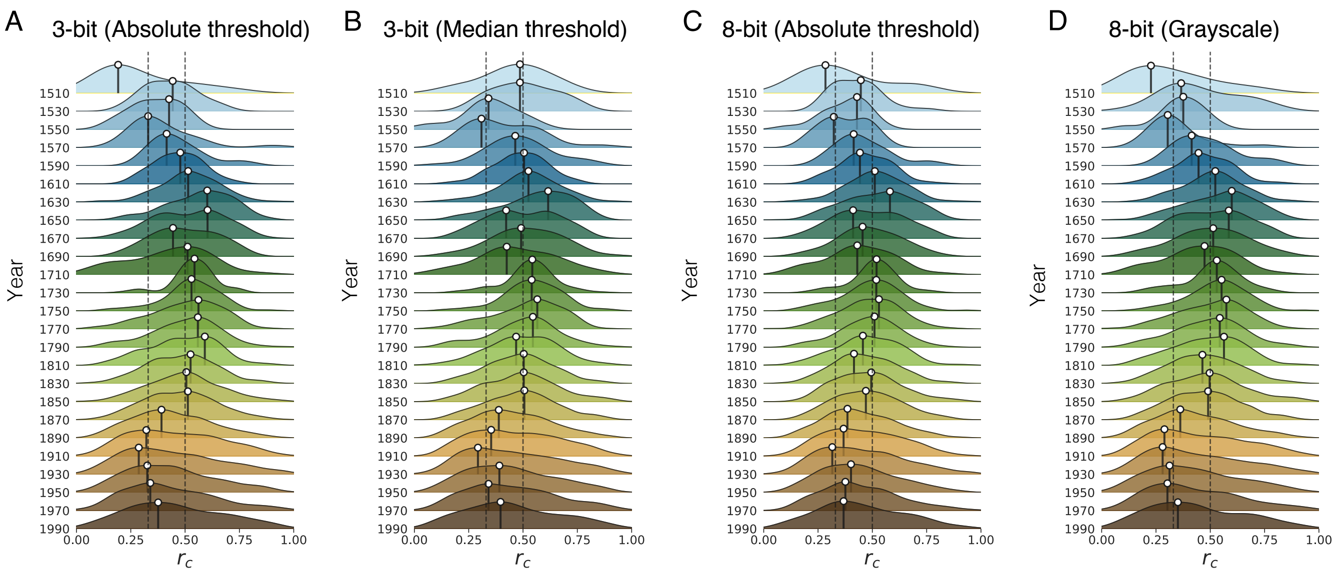

Fig. S11. Distribution of partition ratio r_c for 20-year time window from 1500 to 2000 CE measured from different color depth: (A) 3-bit (absolute threshold), (B) 3-bit (median threshold), (C) 8-bit (absolute threshold), and (D) 8-bit grayscale. The overall trend is similar under different color depth condition.

A B

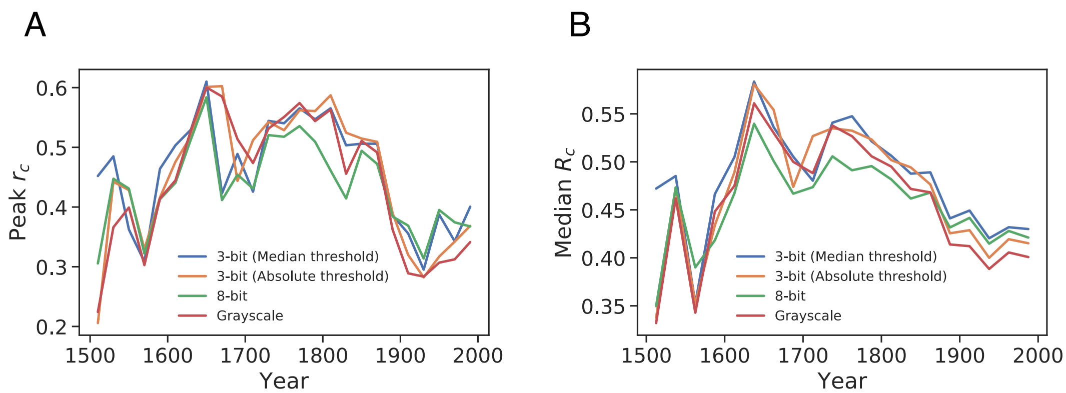

Fig. S12. Change of (A) peak and (B) median r_c obtained from the distribution of partition ratio over time measured from different color depth. The overall trend is similar under different color depth condition.

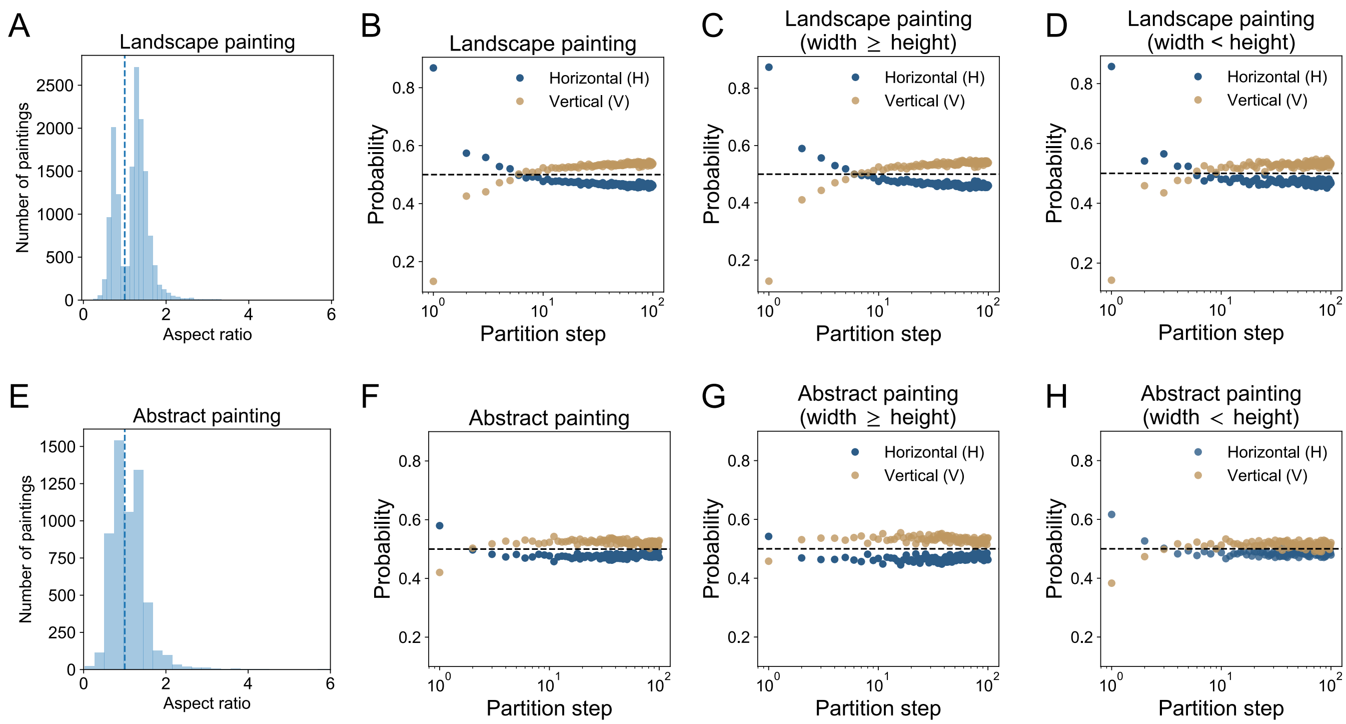

Fig. S13. (A) Aspect ratio distribution of landscape paintings. Proportion of horizontal and vertical partition in each partition step for (B) entire landscape paintings, (C) landscape paintings whose width is longer than the height, and (D) landscape paintings whose height is longer than the width. (E) Aspect ratio distribution of abstract paintings. Proportion of horizontal and vertical partition in each partition step for entire abstract paintings (F), abstract paintings whose width is longer than the height (G), and whose height is longer than the width (H).

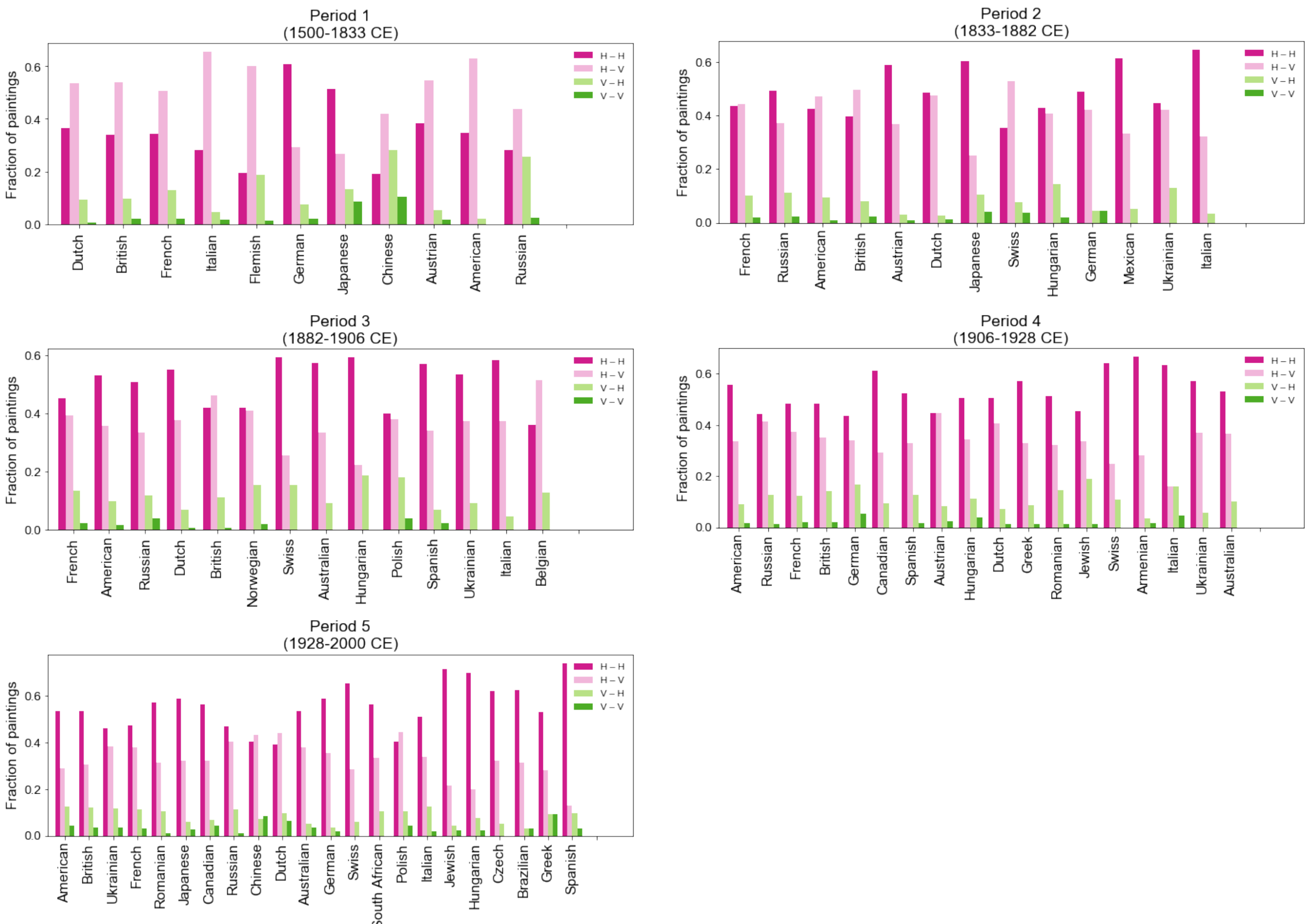

Fig. S14. Distributions of partition types of the dominant individual nationalities with more than 30 paintings for 5 time periods.

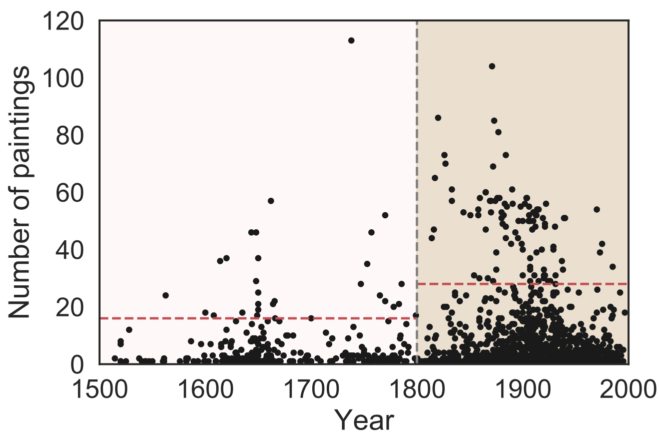

Fig. S15. Number of paintings by individual artists. The number of paintings of individual painters largely increases from 1800 CE. Red line indicates the criterion for top 10% of individuals in each time period who have the largest number of paintings.

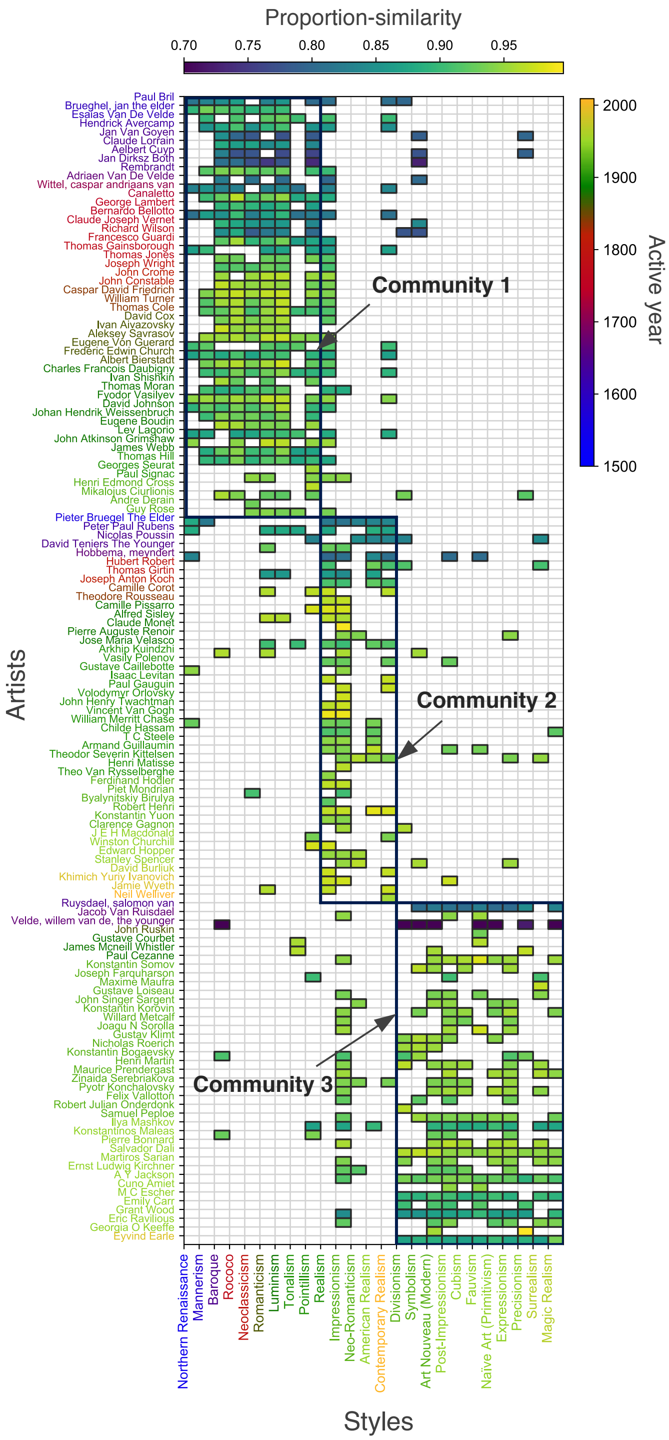

Fig. S16. The enlarged version of Fig. 4A in the main manuscript. Clustering structure in the bipartite proportion-similarity network of individual artists and conventional styles. Colors in the tick labels indicate active year of individual and style periods.

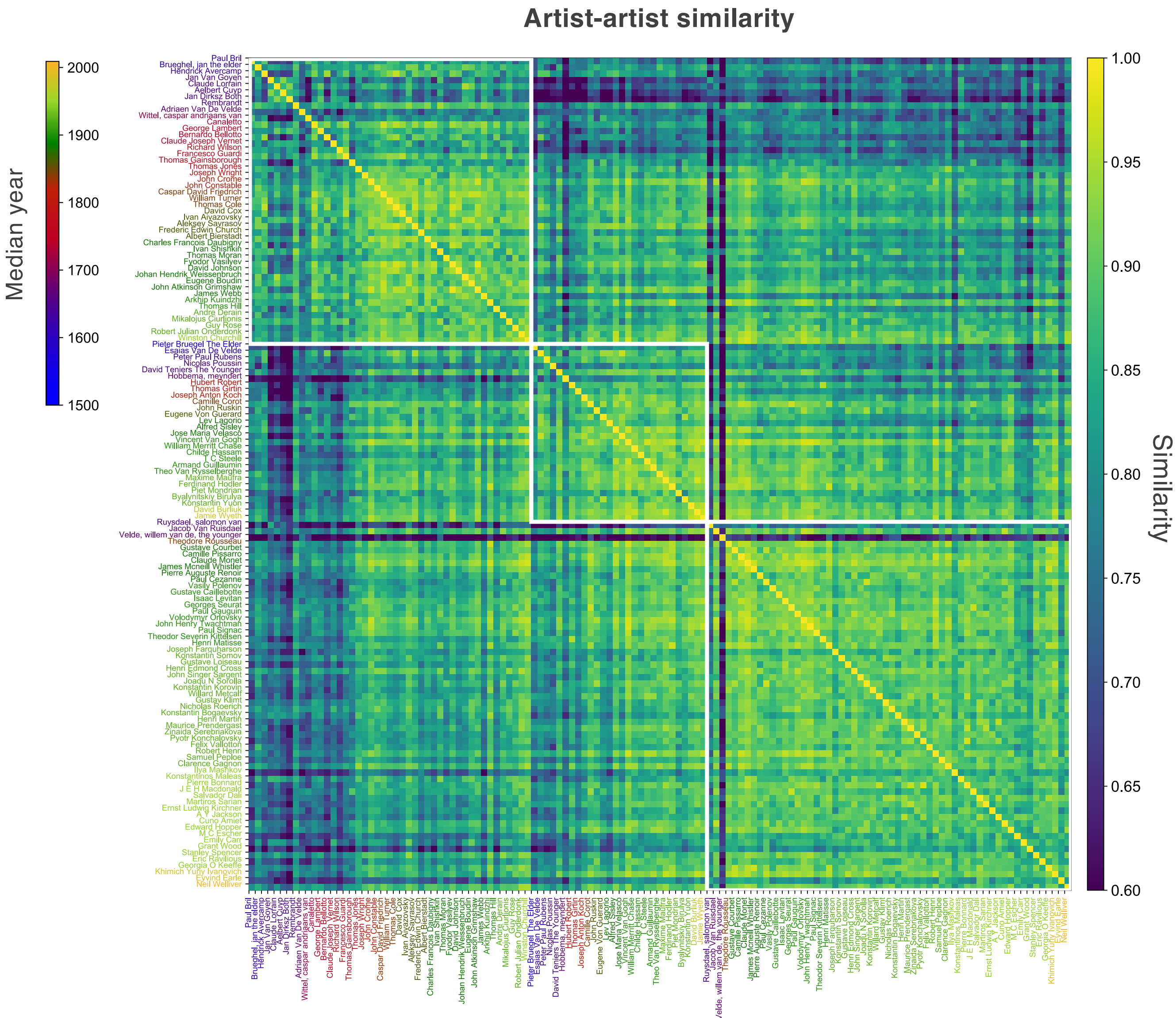

Fig. S17. The enlarged version of Fig. 4C in the main manuscript. Colors in the tick labels indicate median year of each individual.

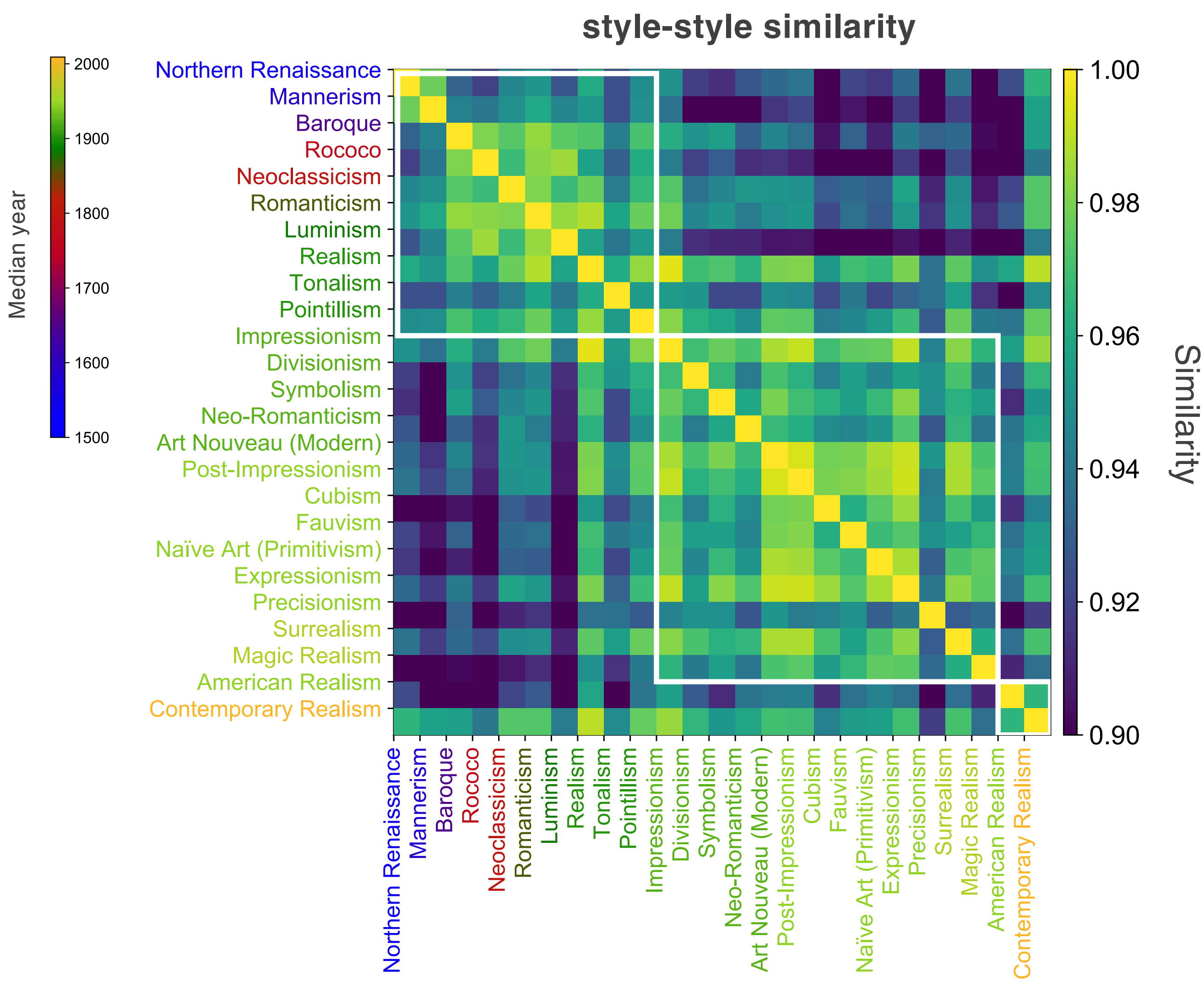

Fig. S18. The enlarged version of Fig. 4D in the main manuscript. Colors in the tick labels indicate median year of paintings in each style period.

Table S2. List of artists in the three communities in the artist-style bipartite network in Fig. 4A in the main manuscript.

Index	Community 1	Community 2	Community 3
1	Paul Bril	Pieter Brugel the Elder	Saloman van Ruysdael
2	Brueghel, Jan the elder	Peter Paul Rubens	Jacob van Ruisdaeal
3	Esaias Van de Velde	Nicolas Poussin	Weillem van de Velde the younger
4	Jan Van Goyen	David Teniers the Younger	John Ruskin
5	Claude Lorrain	Hobbema, meyndert	Gustave Courbet
6	Aelbert Cuyp	Hubert Robert	James Mcneill Whistler
7	Jan Dirksz Both	Thomas Girtin	Paul Cezanne
8	Rembrant	Joseph Anton Koch	Konstantin Somov
9	Adriaen Van De Velde	Camille Corot	Joseph Farquharson
10	Caspar andriaans van Wittel	Theodore Rousseau	Maxime Maufra
11	Canaletto	Camille Pissarro	Gustave Loiseau
12	George Lambert	Alfred Sisley	John Singer Sargent
13	Bernardo Bellotto	Claude Monet	Konstantin Korovin
14	Claude Joseph Vernet	Pierre Auguste Renoir	Willard Metcalf
15	Richard Wilson	Jose Maria Velasco	Joaqu N Sorolla
16	Francesco Guardi	Arkhip Kuindzhi	Gustav Klimt
17	Thomas Gainsborough	Vasily Polenov	Nicholas Roerich
18	Thomas Jones	Gustave Caillebotte	Konstantin Bogaevsky
19	Joseph Wright	Isaac Levitan	Henri Martin
20	John Crome	Paul Gauguin	Maurice Prendergast
21	John Constable	Volodynmyr Orlovsky	Jinaida Serebriakova
22	Caspar David Friedrich	John Henry Twachtman	Pyotr Konchalovsky
23	William Turner	Vincent van Gogh	Felix Vallotton
24	Thomas Cole	William Merritt Chase	Robert Julian Onderdonk
25	David Cox	Childe Hassam	Samuel Peploe
26	Ivan Aivazovsky	T C Steele	Ilya Mashkov
27	Aleksey Savrasov	Armand Guillaumin	Konstantinos Maleas
28	Eugene Von Guerard	Teodor Severin Kittelsen	Pierre Bonnard
29	Frederic Edwin Church	Henri Matisse	Salvador Dali
30	Alebert Bierstadt	Theo van Rysselberghe	Martiros Sarian
31	Charles Francois Daubigny	Ferdinand Hodler	Ernst Ludwig Kirchner
32	Ivan Shishkin	Piet Mondrian	A Y Jackson
33	Thomas Moran	Byalynitskiy Birulya	Cuno Amiet
34	Fyodor Vasilyev	Robert Henri	M C Escher
35	David Johnson	Konstantin Yuon	Emily Carr
36	Johan Hendrik Weissenbruch	Clarence Gagnon	Grant Wood
37	Eugene Boudin	J E H Macdonald	Eric Ravilious
38	Lev Lagorio	Winston Churchill	Georgia O Keeffe
39	John Atkinson Grimshaw	Edward Hopper	Eyvind Earle
40	James Webb	Stanley Spencer	
41	Thomas Hill	David Burliuk	
42	Georges Seurat	Khimich Yuriy Ivanovich	
43	Paul Signac	Jamie Wyeth	
44	Henri Edmond Cross	Neil Welliver	
45	Mikalojus Ciurlionis		
46	Andre Derain		
47	Guy Rose		

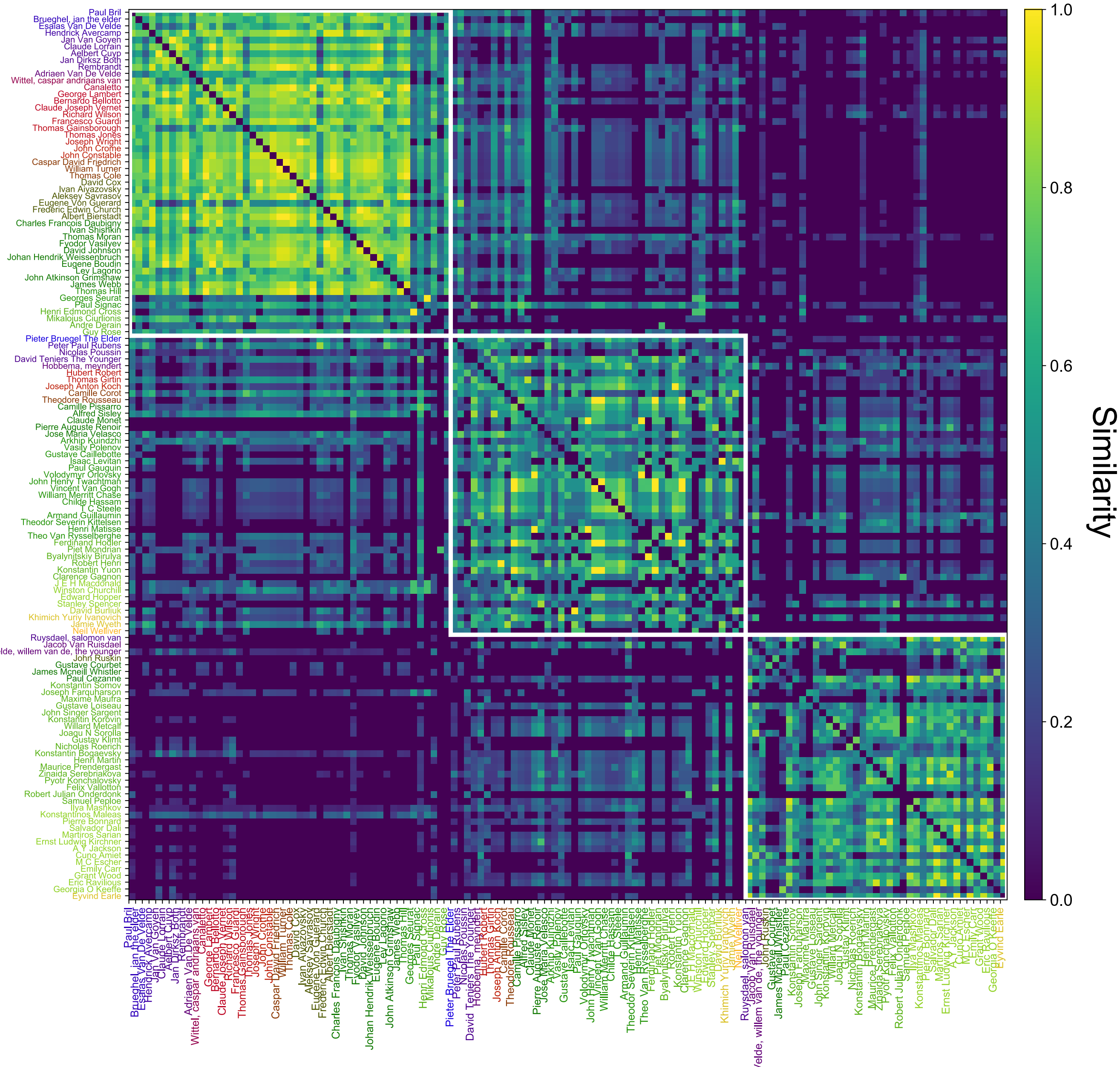

Fig. S19. One-mode projection of the bipartite network (Fig. 4A) onto the individual artists

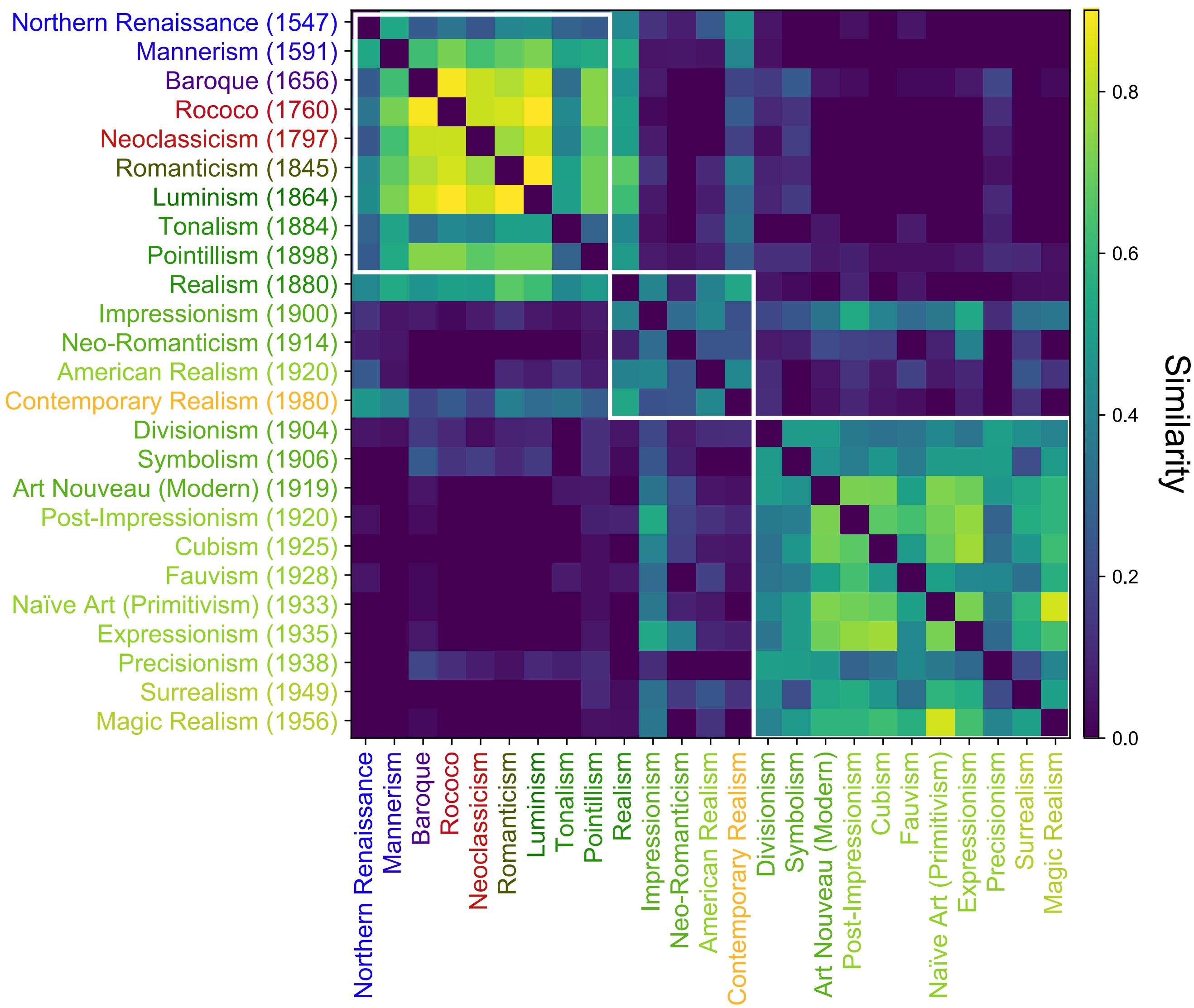

Fig. S20. One-mode projection of the bipartite network (Fig. 4A) onto the conventional style periods

References

1. WikiArt.org - the encyclopedia of painting. Available from: http://www.wikiart.org. (Date of access: 2018-7-17).
2. Krén, E. & Marx, D. Web Gallery of Art. Available from: http://www.wga.hu/. (Date of access: 2018-7-17).
3. Joseph, B., Joseph, I. & Frese, D. PEXELS. Available from: http://www.pexels.com (Date of access: 2018-7-17).
4. https://en.wikipedia.org/ (Date of access: 2020-8-3)
5. https://www.worldcat.org/ (Date of access: 2020-8-3)
6. J. Rigau. M. Feixas, and M. Sbert, IEEE computer graphics and applications 28, 24 (2008).
7. I. S. Shin, S. K. Han, K. M. Lee, S. B. Lee and W. H. Jung, New Phys.: Sae Mulli 63, 655 (2013).